

Astragaloside IV promotes the eNOS/NO/cGMP pathway and improves left ventricular diastolic function in rats with metabolic syndrome

Journal of International Medical Research

48(1) 1–15

© The Author(s) 2019

Article reuse guidelines:

sagepub.com/journals-permissions

DOI: 10.1177/0300060519826848

journals.sagepub.com/home/imr



Xin Lin*, Qiongying Wang* , Shougang Sun, Guangli Xu, Qiang Wu, Miaomiao Qi, Feng Bai and Jing Yu

Abstract

Objectives: This study aimed to explore the effects of astragaloside IV on metabolic syndrome induced by a high-fructose/high-fat diet in rats.

Methods: Rats were randomized into four groups: normal control, metabolic syndrome, metabolic syndrome + intraperitoneal astragaloside 0.5 mg/kg/day, and metabolic syndrome + intraperitoneal astragaloside 2.0 mg/kg/day (n=30 per group) for 14 continuous days. Left ventricular functions were evaluated by hemodynamic and echocardiographic parameters.

Results: Metabolic syndrome rats had a thicker interventricular septum and left ventricular posterior wall, accompanied by a higher E/A wave ratio, reduced E' wave, increased A' wave, decreased E'/A' wave ratio, and higher E/E' wave ratio. Astragaloside decreased insulin and triglyceride levels and improved diastolic dysfunction with no effects on systolic function. A high-fructose/high-fat diet also increased oxidative stress and decreased the myocardial endothelial nitric oxide synthase (NOS) dimer ratio, thus impairing nitric oxide (NO) production and reducing cyclic guanosine monophosphate (cGMP) production. Astragaloside increased NO and cGMP production in the myocardium and improved diastolic function.

Conclusions: Astragaloside alleviated oxidative stress and restored NO signaling, thus improving myocardial left ventricular diastolic dysfunction in rats with metabolic syndrome. The underlying mechanisms could be associated with alleviation of oxidative stress and activation of the endothelial NOS/NO/cGMP pathway.

*These authors contributed equally to this work.

Corresponding author:

Jing Yu, Department of Cardiology, Lanzhou University Second Hospital, No. 82, Chengguan District Lanzhou, Gansu, 730030, China.

Email: yujing2304@126.com

Department of Cardiology, Lanzhou University Second Hospital, Lanzhou, Gansu, China



Creative Commons Non Commercial CC BY-NC: This article is distributed under the terms of the Creative Commons Attribution-NonCommercial 4.0 License (<http://www.creativecommons.org/licenses/by-nc/4.0/>) which permits non-commercial use, reproduction and distribution of the work without further permission provided the original work is attributed as specified on the SAGE and Open Access pages (<https://us.sagepub.com/en-us/nam/open-access-at-sage>).

Keywords

Astragaloside IV, metabolic syndrome, left ventricular diastolic dysfunction, endothelial nitric oxide synthase, oxidative stress, cyclic guanosine monophosphate (GMP)

Date received: 25 October 2018; accepted: 4 January 2019

Introduction

Metabolic syndrome comprises a cluster of commonly co-occurring metabolic disturbances, including insulin resistance, atherogenic dyslipidemia, central obesity, and elevated blood pressure.^{1–3} These disorders, which initially manifest as diastolic dysfunction, are associated with type 2 diabetes mellitus and obesity, and are major risk factors for heart failure.⁴ Patients with metabolic syndrome are therefore at increased risks of cardiovascular events (two-fold increase in cardiovascular outcomes, cardiovascular mortality, myocardial infarction, and stroke) and all-cause mortality (1.5-fold increased risk).^{5,6}

A high-fructose/high-fat diet (HFFD) rat model has been used to study metabolic syndrome.^{7,8} In addition to diet-induced metabolic syndrome models (fructose, sucrose, and high-fat), other models include genetic (*ob/ob* mice, *db/db* mice, Zucker diabetic fatty rats, Otsuka Long-Evans Tokushima fatty rats, and Goto-Kakizaki rats) and chemically-induced models (alloxan and streptozotocin).⁷ All these models present with metabolic syndrome features (hyperinsulinemia, hypertriglyceridemia, and hypertension).⁷ Among the various models, the HFFD model has been widely used for metabolic syndrome research because it of its similar etiology to that observed in clinical metabolic syndrome.^{9–11}

Metabolic syndrome is associated with increased generation of reactive oxygen species (ROS) or reactive nitrogen species.¹² Oxidative stress is generally considered to reflect an imbalance between the

production of ROS and antioxidant capacity. Malondialdehyde (MDA) is an indicator of lipid peroxidation and a marker of oxidative stress.¹³ Superoxide dismutase (SOD) catalyzes the dismutation of superoxide radicals into molecular oxygen or hydrogen peroxide, therefore alleviating oxidative stress.¹⁴ Increased oxidative stress leads to decreased bioavailability of nitric oxide (NO).^{15,16} NO is a ROS scavenger, and increased oxidative stress thus impairs the NO signaling pathway, further limiting the ability of NO to exert its fundamental signaling roles in the cardiovascular system.^{15,16} Previous studies have shown that altered nitric oxide synthase (NOS)/NO signaling is a common feature of metabolic syndrome in animals.^{17–21} Indeed, hypertensive rats with reduced cyclic guanosine monophosphate (cGMP) accumulation and loss of NOS-mediated vasorelaxation also showed reduced NO bioavailability and reduced NO/cGMP signaling in arteriolar vascular smooth muscle cells.^{17–21} Cardiac diastolic dysfunction was recently reported to be associated with NOS uncoupling and cardiac oxidative stress.²²

Astragaloside IV (AST, C₄₁H₆₈O₁₄) is a small molecular saponin and the major active component extracted from *Astragalus membranaceus* (Fisch) BGE. It exhibits multipotent activities under pathophysiological conditions, including anti-hypertensive, positive inotropic, anti-inflammatory, and antioxidant activities.^{23,24} AST has been shown to inhibit the compensatory hypertrophy and apoptosis of myocardial cells after heart failure.²⁵ Zhang et al.²⁶ showed that AST had

favorable effects on lipid metabolism, endothelium-dependent vasodilatation, and the NO/cGMP pathway in a rat model of metabolic syndrome, while another study revealed that AST prevented reperfusion injury through the NO/cGMP/protein kinase G pathway.²⁷ However, the beneficial effects of AST in metabolic syndrome-associated cardiovascular disorders and its underlying mechanisms are still poorly understood.

The present study aimed to explore the effects of AST on blood pressure, left ventricular diastolic function, lipid metabolism, markers of oxidative stress, and the NO signaling pathway in HFFD-induced metabolic syndrome rats.

Methods

Rat models and grouping

The study was approved by the Animal Ethics Committee of Lanzhou University Second Hospital (permit number: 0001191). All animal experiments were performed in accordance with the Guidelines for the Care and Use of Laboratory Animals of the National Institutes of Health. All experiments were performed under sodium pentobarbital anesthesia, and all efforts were made to minimize animal suffering.

Four-week-old male Sprague-Dawley rats were housed at $22\pm 2^{\circ}\text{C}$ in a room equipped with an automatic 12:12-hour photoperiod. Thirty control rats received tap water and standard chow for 24 weeks. The remaining rats received 30% fructose in their drinking water and a high-fat diet for 24 weeks.⁷ The formulae of the standard chow and high-fat diet are shown in Table 1. The amount of water consumed by three rats in each cage was observed every 2 days, and the estimated daily water consumption was 8.3 to 16.7 mL per rat. Rats with a body weight

Table 1. Rat feed formulae and nutritional values.

Ingredient (g/100 g of food)	Standard chow	High-fat diet
Protein	22.10	12.31
Fiber	7.12	2.29
Water	9.20	5.12
Ash	5.20	2.90
Fat	2.28	2.21
Carbohydrate	54.10	30.13
Lard	–	23.04
White granulated sugar	–	10.00
Egg yolk powder	–	10.00
Cholesterol	–	1.50
Cholate	–	0.50
kcal/100 g fodder	353.0	445.7
% Total energy		
Protein	24.7	19.0
Fat	13.8	43.0
Carbohydrate	61.5	38.0

>450 g and fasting blood glucose levels $>6.1\text{ mmol/L}^7$ were considered to have metabolic syndrome and were randomized into three groups ($n=30$ per group): metabolic syndrome group (control metabolic syndrome rats treated with normal saline); metabolic syndrome+AST0.5 group (metabolic syndrome rats treated with intraperitoneal (i.p.) AST 0.5 mg/kg/day); and metabolic syndrome+AST2.0 group (metabolic syndrome rats treated with i.p. AST 2 mg/kg/day). The treatments lasted 14 days. Rats in the normal and metabolic syndrome control groups were injected daily with an equal volume of normal saline for 14 days.

Drug preparation

AST (ChromaDex, Inc., Irvine, CA, USA; purity $>98\%$, high-performance liquid chromatography grade) was supplied as a colorless crystallized powder and was dissolved in 20% dimethylsulfoxide ($<0.05\%$) and diluted with normal saline for use. The chemical structure of AST is shown in Supplementary Figure 1.

Body weight and blood pressure measurements

Rats were weighed after 14 days of treatment (i.e. on the 15th day; similarly herein-after). Systolic blood pressure (SBP) was determined using a standard tail-cuff method with a programmable sphygmomanometer (BP-98A; Softron, Tokyo, Japan). Data were averaged from five recordings.

Transthoracic echocardiography of left ventricular function

After 14 days of treatment, rats were anesthetized with sodium pentobarbital (50 mg/kg, i.p.) to reach a heart rate of around 300 to 350 beats per minute and were then examined by echocardiography (Vivid E9, GE, Pittsburgh, PA, USA; probe i13L Intraoperative Linear Probe). The following parameters were measured: interventricular septal thickness in diastole (IVSd), left ventricular posterior wall thickness in diastole (LVPWd), ejection fraction (EF), fractional shortening (FS), end-systolic left ventricle diameter (LVESD), end-diastolic left ventricle diameter (LVEDD), the wave of mitral inflow from the left atrium to the left ventricle in early-diastole (E wave) velocity, the wave of mitral inflow made by atrial contraction in end-diastole (A wave) velocity, E/A ratio, the wave of mitral annulus movement towards the left atrium in early-diastole during initial filling of the left ventricle (E' wave) velocity, the wave of mitral annulus movement towards the left atrium in end-diastole during late filling of the left ventricle (A' wave) velocity, E'/A' ratio, and E/E' ratio.

Invasive assessment of diastolic dysfunction

Diastolic dysfunction was assessed invasively after 14 days of treatment using a

Mikro-Tip[®] pressure volume catheter and the MPVS Ultra[™] system (both from Millar Instruments, Houston, TX, USA) to assess left ventricular function *in vivo*. Body temperature was maintained at 37°C using a rectal thermometer probe and a DC temperature control module (FHC, New Brunswick, ME, USA). End-systolic left ventricular pressure (LVESP), end-diastolic left ventricular pressure (LVEDP), EF, end-diastolic pressure-volume relationship (EDPVR), +dp/dt max, -dp/dt min, and time constants for isovolumic relaxation (Tau (Glanz)) were measured.

Determination of blood glucose, blood lipids, and serum insulin

Blood was obtained *via* tail prick after the 14 day treatment period and overnight fasting, and glucose levels were measured using a conventional glucometer. After measurement, the rats were anesthetized with sodium pentobarbital (50 mg/kg, i. p.) and blood was collected to measure serum insulin using a rat radioimmunoassay kit (Linco Research, St Charles, MO, USA). Triglycerides (TG), total cholesterol (TC), high-density lipoprotein cholesterol (HDL-C), and low-density lipoprotein cholesterol (LDL-C) were measured using an automatic analyzer (Hitachi, Tokyo, Japan).

Preparation of left ventricular myocardium tissues

After drawing blood (described above), the hearts were removed quickly under anesthesia, and washed with iced phosphate-buffered saline. The left ventricles were then cut into several small pieces (about 30 mg) and put in a liquid nitrogen container (-86°C) for subsequent measurements.

MDA and SOD in the myocardium

Oxidative stress markers, including SOD and MDA, were measured in left ventricular myocardium samples using commercial kits (Nanjing Jiancheng Bioengineering Institute, Nanjing, China) according to the manufacturer's instructions. Coefficients of variation were 1.7% for SOD and 2.3% for MDA.

NO in the myocardium

NO was measured in homogenates of left ventricular tissues using an NO detection kit (Biovision, Mountain View, CA, USA) according to manufacturer's instructions. The optical density values of the samples were measured at 540 nm on a spectrophotometer (Beckman DU530, Beckman Coulter, Brea, CA, USA). NO production in the homogenate was represented by the concentration of total nitrite/nitrate, expressed as $\mu\text{mol}/\text{mg}$ protein. The coefficient of variation was 1.7%.

Tissue cGMP

Left ventricle samples (about 30 mg) were weighed and homogenized in 50 mmol/L cold acetic acid and centrifuged at $13,000 \times g$ for 10 minutes. The precipitate was extracted twice with ethanol (5 minutes each time) and the supernatant was collected for determination of cGMP using a commercial radioimmunoassay kit (Jian Cheng, Nanjing, China). The coefficient of variation was 2.6%.

NOS expression by western blot

NOS protein expression levels, including neuronal NOS (nNOS) and endothelial NOS (eNOS) monomers and dimers, were assayed in left ventricle samples using sodium dodecyl sulfate-polyacrylamide gel electrophoresis western blot analysis under non-reducing and

reducing conditions, respectively. Immunoreactive bands were visualized by enhanced chemiluminescence (Pierce, Rockford, IL, USA). Protein expression was assessed by densitometric analysis using Image J software (National Institutes of Health, Bethesda, MD, USA).

Statistical analysis

All data were expressed as mean \pm standard error of the mean (SEM). Comparisons between two groups were performed with Student's *t*-test. Multiple groups were compared using one-way ANOVA and the Bonferroni post-hoc test. Two-sided *P*-values <0.05 were considered statistically significant. Statistical analyses were performed using SPSS 17 (SPSS Inc., Chicago, IL, USA).

Results

HFFD-induced metabolic syndrome rats showed abnormal glucose and lipid metabolism, and AST improved insulin and TG levels

Fasting blood glucose was significantly higher in HFFD-fed metabolic syndrome rats compared with normal controls ($P < 0.05$). Fasting insulin and TG levels were also significantly higher in metabolic syndrome rats compared with normal control rats (both $P < 0.05$). AST had no effect on fasting blood glucose, but AST 0.5 and 2 mg/kg/day both significantly decreased serum insulin and TG levels compared with control metabolic syndrome rats (all $P < 0.05$) (Table 2). There were no significant differences in TC, HDL-C, and LDL-C levels among normal rats and metabolic syndrome rats with or without AST.

Table 2. Biochemical characteristics of normal and metabolic syndrome rats treated with or without AST.

	NC	Metabolic syndrome	Metabolic syndrome + AST0.5	Metabolic syndrome + AST2.0
FBG (mmol/L)	5.18 ± 0.91	7.88 ± 0.86*	7.37 ± 1.06*	7.38 ± 0.73*
Serum insulin (ng/mL)	1.15 ± 0.19	4.23 ± 0.71*	3.85 ± 0.51* [#]	3.16 ± 0.45* [#]
TG (mmol/L)	1.05 ± 0.32	2.59 ± 0.48*	2.11 ± 0.29* [#]	1.81 ± 0.25* [#]
TC (mmol/L)	1.95 ± 0.52	2.26 ± 0.40	2.03 ± 0.41	2.08 ± 0.42
LDL-C (mmol/L)	0.45 ± 0.07	0.47 ± 0.06	0.43 ± 0.07	0.43 ± 0.08
HDL-C (mmol/L)	1.17 ± 0.18	1.21 ± 0.29	1.21 ± 0.24	1.16 ± 0.19

AST: astragaloside IV, NC: normal control, FBG: fasting blood glucose, TG: triglycerides, TC: total cholesterol, LDL-C: low-density lipoprotein cholesterol, HDL-C: high-density lipoprotein cholesterol.

Data presented as mean ± SEM (n=30 per group). * $P < 0.05$ vs. NC group; [#] $P < 0.05$ vs. metabolic syndrome group.

HFFD-induced metabolic syndrome caused left ventricular diastolic dysfunction, which could be attenuated by AST

There were no major differences in EF and FS among all the groups, and little change in systolic performance according to transthoracic echocardiography in rats with HFFD-induced metabolic syndrome (Table 3). However, metabolic syndrome rats showed slight increases in IVSd and LVPWd, determined by M-mode imaging (both $P < 0.05$; Figure 1a, Table 3). These were reduced by AST treatment, but the differences were not significant (Table 3). Regarding mitral inflow pulse-wave and tissue Doppler imaging (Figure 1b–e), for mitral inflow from the left atrium to the left ventricle, the velocity ratio E/A increased markedly in metabolic syndrome rats ($P < 0.05$) and was restored to normal levels by high-dose AST (2.0 mg/kg) (Figure 1b and d, Table 3), while metabolic syndrome rats also showed a significant reduction in E' and rise in A', resulting in a decreased E'/A' ratio ($P < 0.05$), all of which were significantly improved by AST (Figure 1c and e, Table 3). The velocity E/E' ratio has been reported to show the strongest correlation with invasive

hemodynamic measures of diastolic dysfunction.²² Metabolic syndrome rats had a significantly higher E/E' ratio compared with normal control rats ($P < 0.05$), and this ratio was reduced to normal by high-dose AST (Figure 1f, Table 3).

Invasive hemodynamic evaluation showed that LVESP, LVEDP, and EDPVR were all significantly elevated and the Tau (Glantz) was significantly prolonged in metabolic syndrome rats compared with controls (all $P < 0.05$). All these diastolic parameters were restored by high-dose AST (Table 4).

AST did not control high SBP in HFFD-induced metabolic syndrome rats

After 14 days of treatment, rat body weights were increased by 17%, 18%, and 16% in the metabolic syndrome, metabolic syndrome+AST0.5, and metabolic syndrome+AST2.0 groups, respectively (all $P < 0.05$) (Figure 2a). SBP was significantly higher in the HFFD-induced metabolic syndrome rats compared with control rats ($P < 0.05$) (Figure 2b). AST administration had no obvious effect on body weight changes and SBP in metabolic syndrome rats.

Table 3. Transthoracic echocardiography measurements in normal and metabolic syndrome rats treated with or without AST.

	NC	Metabolic syndrome	Metabolic syndrome + AST0.5	Metabolic syndrome + AST2.0
M-mode imaging of left ventricle				
IVSd (mm)	1.14 ± 0.14	1.36 ± 0.20*	0.34 ± 0.18	1.26 ± 0.11
LVPWd (mm)	1.35 ± 0.18	1.74 ± 0.24*	1.50 ± 0.21	1.49 ± 0.18
LVESD (mm)	3.54 ± 0.46	3.77 ± 0.65	3.60 ± 0.62	3.87 ± 0.48
LVEDD (mm)	5.91 ± 0.49	6.01 ± 0.75	6.04 ± 0.82	6.17 ± 0.45
EF (%)	76.4 ± 6.0	75.9 ± 6.2	76.9 ± 5.7	72.6 ± 7.7
FS (%)	40.6 ± 5.3	40.0 ± 6.3	40.7 ± 5.6	37.1 ± 5.8
Pulse-wave Doppler imaging for measuring mitral inflow velocities				
E wave velocity (mm/s)	705 ± 90	717 ± 45	673 ± 78	642 ± 61
A wave velocity (mm/s)	543 ± 90	288 ± 57*	423 ± 90 [#]	453 ± 53 [#]
E/A ratio	1.31 ± 0.15	2.57 ± 0.53*	1.64 ± 0.27* [#]	1.44 ± 0.26 [#]
Tissue Doppler imaging for measuring septal mitral annulus velocities				
E' wave velocity (mm/s)	40.9 ± 4.9	25.7 ± 3.0*	28.4 ± 2.1*	33.1 ± 3.3* [#]
A' wave velocity (mm/s)	27.2 ± 6.0	38.6 ± 4.7*	27.8 ± 3.7 [#]	26.8 ± 3.9 [#]
E'/A' ratio	1.55 ± 0.31	0.67 ± 0.08*	1.04 ± 0.18* [#]	1.24 ± 0.16* [#]
E/E' ratio	17.3 ± 1.1	28.1 ± 2.7*	23.8 ± 2.7* [#]	19.5 ± 2.3 [#]

AST: astragaloside IV, NC: normal control, IVSd: interventricular septal thickness in diastole, LVPWd: left ventricular posterior wall thickness in diastole, EF: ejection fraction, FS: fractional shortening, LVESD: end-systolic left ventricle diameter, LVEDD: end-diastolic left ventricle diameter, E wave: wave of mitral inflow from left atrium to left ventricle in early-diastole, A wave: wave of mitral inflow made by atrial contraction in end-diastole, E' wave: wave of mitral annulus movement towards left atrium in early-diastole, during initial filling of left ventricle, A' wave: wave of mitral annulus movement towards left atrium in end-diastole, during late filling of left ventricle.

Data presented as mean ± SEM (n=7 per group). **P* < 0.05 vs. NC group; [#]*P* < 0.05 vs. metabolic syndrome group.

HFFD-induced metabolic syndrome increased oxidative stress, which was reduced by AST

MDA levels were increased and SOD levels were decreased by HFFD (both *P* < 0.05) (Figure 3). AST treatment restored SOD levels (*P* < 0.05) but had no significant effect on MDA levels.

HFFD-induced metabolic syndrome decreased myocardial eNOS dimer expression, which was increased by AST

Total eNOS and nNOS expression levels were unaffected by HFFD or AST (Figure 4a). However, the eNOS dimer/

monomer ratio was significantly decreased in metabolic syndrome rats compared with normal controls (*P* < 0.05; Figure 4b and 4c), but there was no significant change in the nNOS dimer/monomer ratio (Figure 4b and d). Compared with metabolic syndrome rats, AST (0.5 and 2.0 mg/kg) significantly increased the eNOS dimer/monomer ratio in the myocardium (both *P* < 0.05; Figure 4b and c).

HFFD-induced metabolic syndrome decreased NO and cGMP levels, and AST restored NO signaling

The total NO content of the left ventricular myocardium was significantly lower in

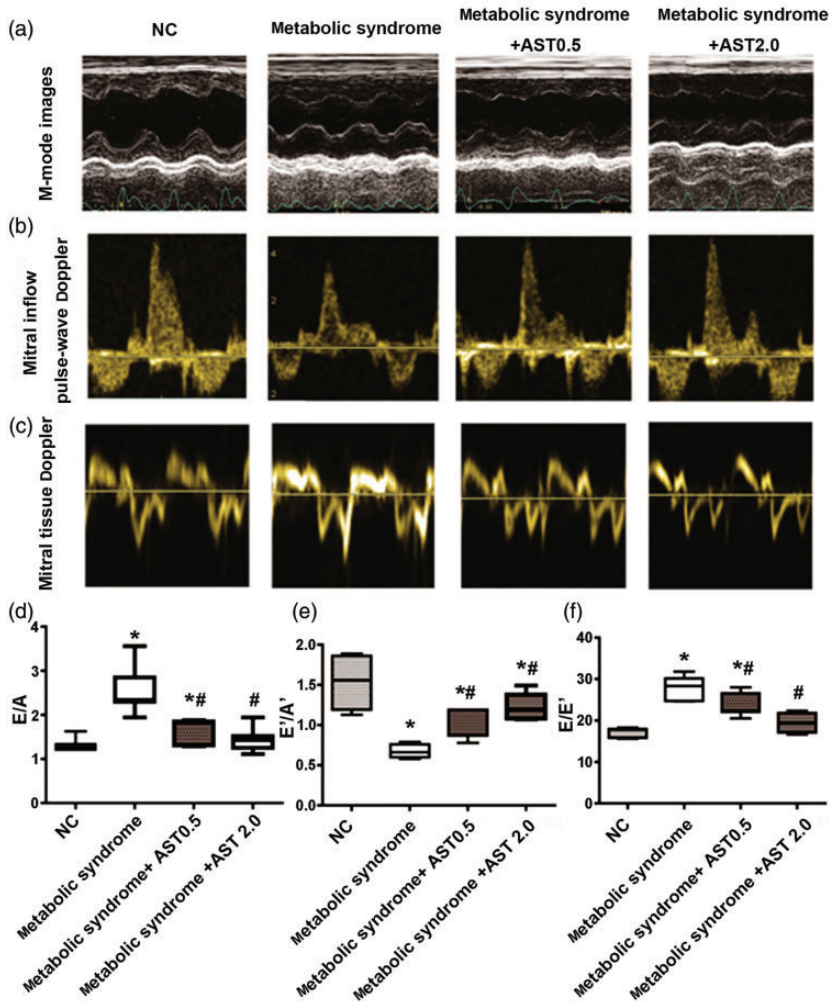


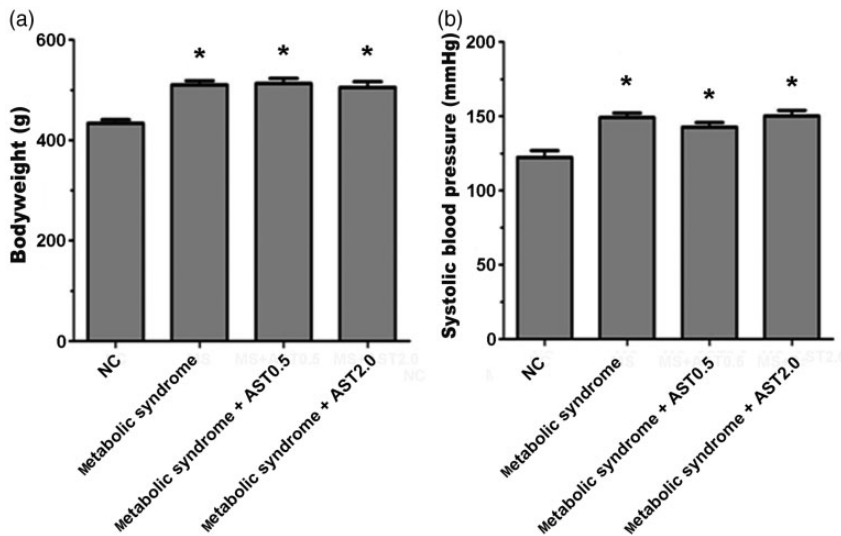
Figure 1. Transthoracic echocardiographic parameters in normal and metabolic syndrome rats treated with or without AST. Representative images of (a) M-mode imaging of left ventricle obtained at mid-papillary level in parasternal long-axis view; (b) pulse-wave Doppler imaging of mitral inflow; and (c) tissue Doppler imaging of septal mitral annulus movement. (d) Mitral inflow velocities calculated based on pulse-wave Doppler imaging. Velocity ratio of E wave (wave of mitral inflow from left atrium to left ventricle in early-diastole) to A wave (wave of mitral inflow by atrial contraction in end-diastole). (e) Septal mitral annulus longitudinal velocities calculated based on tissue Doppler imaging. Velocity ratio of E' wave (wave of mitral annulus movement towards left atrium in early-diastole during initial filling of left ventricle) to A' wave (wave of mitral annulus movement towards left atrium in end-diastole during late filling of the left ventricle). (f) Ratio of E wave to E' wave velocity. NC: normal control, AST: astragaloside IV. Data presented as mean \pm SEM (n = 7). *P < 0.05 vs. NC group; #P < 0.05 vs. metabolic syndrome group.

Table 4. Invasive hemodynamic measurements in normal and metabolic syndrome rats treated with or without AST.

	NC	Metabolic syndrome	Metabolic syndrome + AST0.5	Metabolic syndrome + AST2.0
HR (bpm)	367 ± 28	372 ± 41	377 ± 34	374 ± 46
Systolic index				
+dp/dt max (mmHg/s)	10,304 ± 107	10,270 ± 132	10,666 ± 736	10,272 ± 221
LVESP (mmHg)	136 ± 6	157 ± 9*	154 ± 8*	154 ± 13*
EF (%)	71.0 ± 4.9	69.3 ± 6.8	71.8 ± 7.2	67.0 ± 9.6
Diastolic index				
-dp/dt min (mmHg/s)	8487 ± 286	8364 ± 217	8535 ± 324	8465 ± 224
LVEDP (mmHg)	6.88 ± 0.96	10.28 ± 0.94*	8.37 ± 1.32*	8.22 ± 0.72 [#]
EDPVR (mmHg/μL)	0.25 ± 0.06	0.45 ± 0.07*	0.38 ± 0.07*	0.33 ± 0.08 [#]
Tau (Glanz) (ms)	10.27 ± 1.26	15.05 ± 0.99*	13.00 ± 1.02* [#]	12.93 ± 1.27* [#]

AST: astragaloside IV, NC: normal control, HR: heart rate, LVESP: end-systolic left ventricular pressure, LVEDP: end-diastolic left ventricular pressure, EF: ejection fraction, EDPVR: end-diastolic pressure-volume relationship, Tau (Glanz): time constants for isovolumic relaxation.

Data presented mean ± SEM (n=7 per group). *P < 0.05 vs. NC group; [#]P < 0.05 vs. metabolic syndrome group.

**Figure 2.** Body weight and systolic blood pressure of normal and metabolic syndrome rats treated with or without AST. (a) Bodyweight and (b) systolic blood pressure in normal control rats, metabolic syndrome rats, and metabolic syndrome rats treated with AST 0.5 or 2.0 mg/kg.

AST: astragaloside IV, NC: normal control. Data shown as mean ± SEM (n = 12). *P < 0.05 vs. NC group.

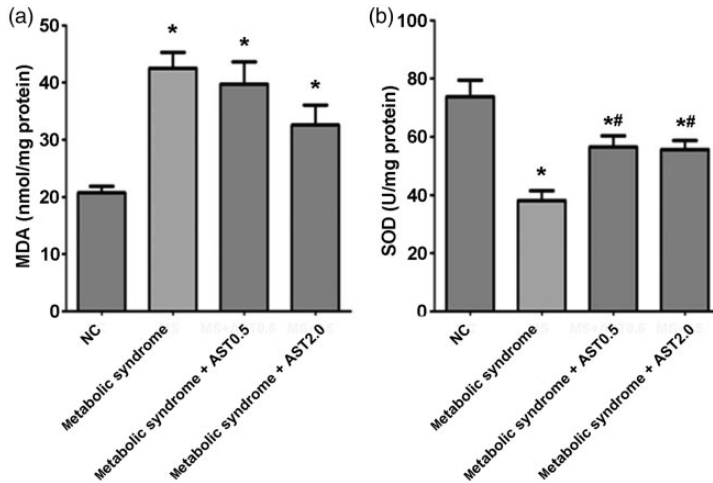


Figure 3. Oxidative stress markers in the left ventricular myocardium of normal and metabolic syndrome rats treated with or without AST. (a) MDA and (b) SOD activity in the myocardium.

AST: astragaloside IV, NC: normal control, MDA: malondialdehyde, SOD: superoxide dismutase. Data presented as mean \pm SEM ($n = 12$). * $P < 0.05$ vs. NC group; # $P < 0.05$ vs. metabolic syndrome group.

metabolic syndrome rats compared with controls ($P < 0.05$) (Figure 4e). Both AST treatments increased NO levels (both $P < 0.05$), with high-dose AST being more effective. Similar results were observed for cGMP (Figure 4f).

Discussion

Metabolic syndrome manifesting as diastolic dysfunction is a risk factor for heart failure.^{28,29} AST is known to have protective effects on cardiac function, but its effects on metabolic syndrome-induced cardiac dysfunction are poorly known. The current study showed that AST improved myocardial left ventricular diastolic dysfunction in HFFD-induced metabolic syndrome rats, via mechanisms associated with alleviation of oxidative stress and activation of the eNOS/NO/cGMP pathway.

The present results showed that AST could relieve some features of metabolic syndrome, such as hyperinsulinemia and dyslipidemia, as indicated by a previous study.²⁶ Although AST 2.0 mg/kg had a

more notable effect than AST 0.5 mg/kg, it was not possible to establish a clear dose-dependent relationship because only two doses were used. These results suggest that AST could play a potential role in the treatment of HFFD-induced metabolic abnormalities. However, further studies are needed to investigate the histology of the heart, liver, and adipose tissue, as well as the mechanisms underlying the effects of AST in improving glucose and lipid metabolic alterations.

In the present study, AST alleviated heart dysfunction induced by HFFD, as supported by a previous study.²⁶ In addition, HFFD-fed rats exhibited mild hypertension, possibly as a result of the increased salt intake and weight gain. Multiple pathways are involved in the pathogenesis of metabolic syndrome-associated diastolic dysfunction, including hypertension, inflammation, and obesity. In the present study, AST had no effect on SBP, suggesting that the AST-induced improvements in diastolic function were due to mechanisms other than improved blood pressure. AST

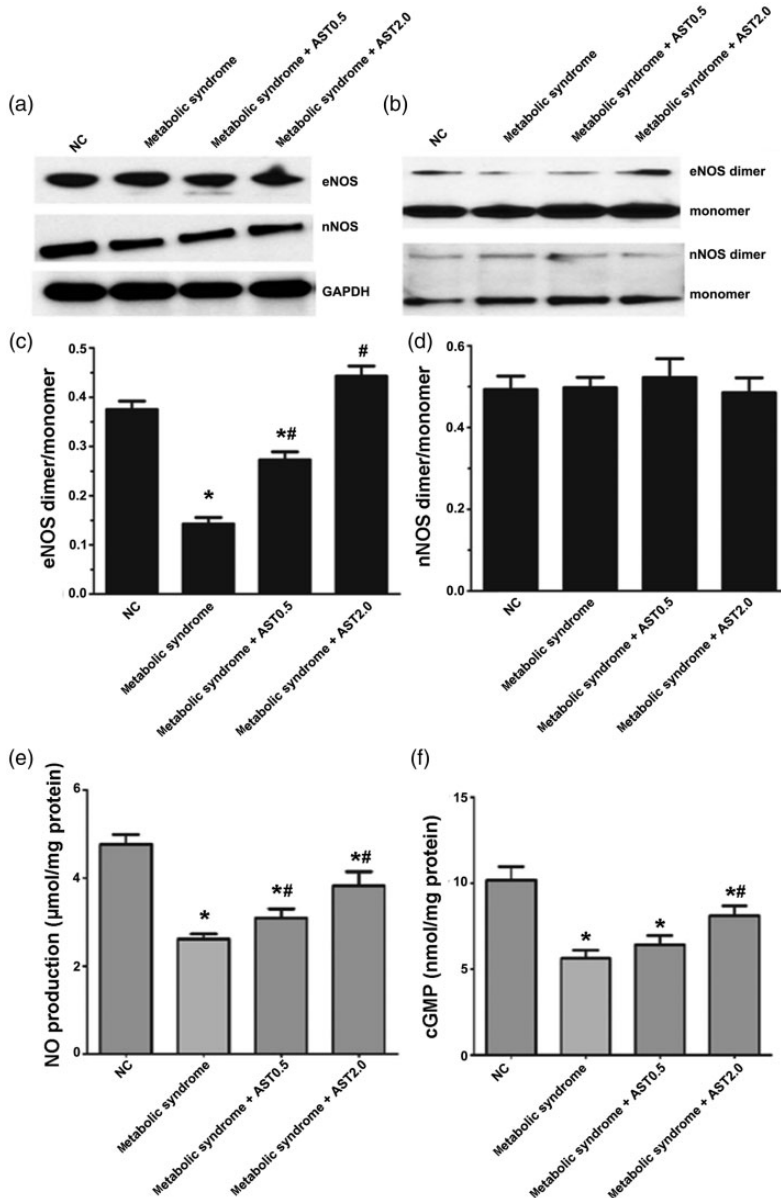


Figure 4. Changes in NO signaling in normal and metabolic syndrome rats treated with or without AST. Representative images of western blots for (a) total eNOS and nNOS and (b) eNOS and nNOS dimers and monomers. (c) Ratios of eNOS and (d) nNOS dimers to monomers. (e) Total NO production normalized to protein content from the corresponding well. (f) cGMP levels in myocardium.

NO: nitric oxide, AST: astragaloside IV, eNOS: endothelial nitric oxide synthase, nNOS: neuronal nitric oxide synthase, NC: normal control. Data expressed as mean \pm SEM ($n = 6$ for a–d; $n = 12$ for e, f). * $P < 0.05$ vs. NC group; # $P < 0.05$ vs. metabolic syndrome group.

scavenges oxygen free radicals generated from the injured myocardium, and ROS interfere with the Ca^{2+} transport systems across the sarcoplasmic reticulum membrane.^{30,31} We hypothesize that AST may improve sarcoplasmic reticulum function and Ca^{2+} handling by cardiomyocytes, ultimately benefiting diastolic function. However, the limited study of the effects of oxidative stress and metabolic abnormalities on blood glucose, lipids, and body weight means that further studies are needed to explore the contributions of salt and inflammation to diastolic dysfunction in metabolic syndrome rats. In addition, the current study did not measure obesity-related indicators such as wet weight of abdominal fat pads and dual-energy X-ray absorptiometry measurements, or inflammation markers, which will be examined in future studies.

The present results showed that AST could increase NO and cGMP production in the myocardium, coincident with improved diastolic function. In the cardiovascular system, eNOS induces endothelium-dependent vasodilatation and regulates intracellular Ca^{2+} handling and β -adrenergic receptor signaling.³² AST influences cardiac inotropic responses and peripheral vascular resistance, and NO/cGMP probably play a major role in these effects.^{33,34} Myocardial homogenates from patients with heart failure but preserved ejection fraction were recently shown to have low cGMP levels.³⁵ Deficient NO-cGMP-PKG signaling from the endothelium to the myocardium has also been shown to affect myocardial relaxation in isolated cardiac myocytes.³⁶

Diet-induced metabolic syndrome is associated with oxidative stress.^{37,38} SOD activity is decreased in patients with metabolic syndrome, while MDA, C-reactive protein, and xanthine oxidase levels are increased, indicating oxidative stress.³⁹ The results of the present study showed

that NO production and SOD levels were decreased and MDA levels were increased in the left ventricular myocardium in HFFD-fed metabolic syndrome rats. Furthermore, AST treatment attenuated cardiac MDA levels and enhanced NO production and SOD levels, suggesting that relief of oxidative stress could help to explain the AST-induced improvements in glucose and lipid metabolism.⁴⁰⁻⁴²

To clarify the relationship between oxidative stress and diastolic dysfunction in HFFD-induced metabolic syndrome rats, we examined the expression levels of eNOS and nNOS, and their dimerization. Increased NOS uncoupling may play a role in increased oxidative stress, as well as diminished energy use in myocardial diastolic functions.²² In the present study, eNOS dimerization was markedly decreased in HFFD-induced metabolic syndrome rats, and this effect was partly reversed by AST. The improved diastolic function and reduced oxidative stress in metabolic syndrome rats treated with AST suggest that AST may mitigate cardiac diastolic dysfunction and oxidative stress by accelerating the production of antioxidant molecules in the myocardium. Limiting the accumulation of ROS by improving NO delivery has been shown in the *db/db* rat model of insulin resistance and in patients, thus emphasizing the pivotal importance of oxidative stress and alterations in vascular structure and diastolic dysfunction in metabolic syndrome.^{43,44} eNOS dimerization is necessary for the regulation of NO production during oxidative stress.⁴⁵ Changes in the eNOS dimer to monomer ratio could modulate its function in diabetes and myocardial infarction.⁴⁶ The present study showed significantly decreased eNOS dimers in metabolic syndrome rats, consistent with the previous studies presented above.

Although the present results strongly suggested that AST restored the

eNOS/NO/cGMP pathway in HFFD-fed metabolic syndrome rats, we could not determine if this effect was the sole or primary mechanism underlying the improvement in left ventricular diastolic dysfunction. We only examined the role of oxidative stress, and alternative signaling pathways may explain some of the disparate effects, such as the reversed hypertriglyceridemia and hyperinsulinemia without changes in blood pressure, glucose, and weight gain. Additional studies are therefore required to determine the exact mechanisms involved in the beneficial effects of AST in metabolic syndrome.

In conclusion, the results of the present study suggest that AST could alleviate the oxidative stress and metabolic abnormalities associated with metabolic syndrome in rats, and could protect left ventricular diastolic function. The beneficial effects of AST may be mediated by the eNOS/NO/cGMP pathway.

Acknowledgments

The authors thank Dr. Peng Chang, Dr. Xiuli Li, and Dr. Ningyin Li for donating the reagents and materials for this study. All authors thank Dr. Ganesh Paudel for reviewing and modifying this manuscript.

Declaration of conflicting interest

The authors declare that there is no conflict of interest.

Funding

This study was supported by the Health Commission of Gansu Province Foundation (GZK-2018-51 and GWSKY2018-19), the Foundation of Lanzhou University Second Hospital (ynbskyjj2015-1-11, ynbskyjj2016-2-1, and sdkyjj2016-10), the Cuiying Scientific and Technological Innovation Program of Lanzhou University Second Hospital (CY2017-MS14), and the Cuiying Graduate Supervisor

Applicant Training Program of Lanzhou University Second Hospital.

ORCID iD

Qiongying Wang  <http://orcid.org/0000-0002-5497-3196>

References

1. Alberti KG, Eckel RH, Grundy SM, et al. Harmonizing the metabolic syndrome: a joint interim statement of the International Diabetes Federation Task Force on Epidemiology and Prevention; National Heart, Lung, and Blood Institute; American Heart Association; World Heart Federation; International Atherosclerosis Society; and International Association for the Study of Obesity. *Circulation* 2009; 120: 1640–1645.
2. Samson SL and Garber AJ. Metabolic syndrome. *Endocrinol Metab Clin North Am* 2014; 43: 1–23.
3. Kim CJ, Park J and Kang SW. Prevalence of metabolic syndrome and cardiovascular risk level in a vulnerable population. *Int J Nurs Pract* 2015; 21: 175–183.
4. Alba AC, Agoritsas T, Jankowski M, et al. Risk prediction models for mortality in ambulatory patients with heart failure: a systematic review. *Circ Heart Fail* 2013; 6: 881–889.
5. Mottillo S, Filion KB, Genest J, et al. The metabolic syndrome and cardiovascular risk: a systematic review and meta-analysis. *J Am Coll Cardiol* 2010; 56: 1113–1132.
6. Said S, Mukherjee D and Whayne TF. Interrelationships with metabolic syndrome, obesity and cardiovascular risk. *Curr Vasc Pharmacol* 2016; 14: 415–425.
7. Alexandre de Artinano A and Miguel Castro M. Experimental rat models to study the metabolic syndrome. *Br J Nutr* 2009; 102: 1246–1253.
8. Panchal SK, Poudyal H, Iyer A, et al. High-carbohydrate, high-fat diet-induced metabolic syndrome and cardiovascular remodeling in rats. *J Cardiovasc Pharmacol* 2011; 57: 611–624.
9. Wang O, Liu J, Cheng Q, et al. Effects of ferulic acid and gamma-oryzanol on high-fat

- and high-fructose diet-induced metabolic syndrome in rats. *PLoS One* 2015; 10: e0118135.
10. Zhang J, Wang O, Guo Y, et al. Effect of increasing doses of linoleic and alpha-linolenic acids on high-fructose and high-fat diet induced metabolic syndrome in rats. *J Agric Food Chem* 2016; 64: 762–772.
 11. Zhang J, Zhao L, Cheng Q, et al. Structurally different flavonoid subclasses attenuate high-fat and high-fructose diet induced metabolic syndrome in rats. *J Agric Food Chem* 2018; 66: 12412–12420.
 12. Carrier A. Metabolic syndrome and oxidative stress: a complex relationship. *Antioxid Redox Signal* 2017; 26: 429–431.
 13. Yara S, Lavoie JC and Levy E. Oxidative stress and DNA methylation regulation in the metabolic syndrome. *Epigenomics* 2015; 7: 283–300.
 14. Culotta VC. Superoxide dismutase, oxidative stress, and cell metabolism. *Curr Top Cell Regul* 2000; 36: 117–132.
 15. Magenta A, Greco S, Capogrossi MC, et al. Nitric oxide, oxidative stress, and p66Shc interplay in diabetic endothelial dysfunction. *Biomed Res Int* 2014; 2014: 193095.
 16. Schiffrin EL. Oxidative stress, nitric oxide synthase, and superoxide dismutase: a matter of imbalance underlies endothelial dysfunction in the human coronary circulation. *Hypertension* 2008; 51: 31–32.
 17. Aroor AR, McKarns S, Demarco VG, et al. Maladaptive immune and inflammatory pathways lead to cardiovascular insulin resistance. *Metabolism* 2013; 62: 1543–1552.
 18. Du J, Fan LM, Mai A, et al. Crucial roles of Nox2-derived oxidative stress in deteriorating the function of insulin receptors and endothelium in dietary obesity of middle-aged mice. *Br J Pharmacol* 2013; 170: 1064–1077.
 19. Pakdeechote P, Bunbupha S, Kukongviriyapan U, et al. Asiatic acid alleviates hemodynamic and metabolic alterations via restoring eNOS/iNOS expression, oxidative stress, and inflammation in diet-induced metabolic syndrome rats. *Nutrients* 2014; 6: 355–370.
 20. Dou J, Li H, Ma X, et al. Osteocalcin attenuates high fat diet-induced impairment of endothelium-dependent relaxation through Akt/eNOS-dependent pathway. *Cardiovasc Diabetol* 2014; 13: 74.
 21. Fellner SK and Arendshorst WJ. Complex interactions of NO/cGMP/PKG systems on Ca²⁺ signaling in afferent arteriolar vascular smooth muscle. *Am J Physiol Heart Circ Physiol* 2010; 298: H144–H151.
 22. Silberman GA, Fan TH, Liu H, et al. Uncoupled cardiac nitric oxide synthase mediates diastolic dysfunction. *Circulation* 2010; 121: 519–528.
 23. Wang C, Li Y, Yang X, et al. Tetramethylpyrazine and astragaloside IV synergistically ameliorate left ventricular remodeling and preserve cardiac function in a rat myocardial infarction model. *J Cardiovasc Pharmacol* 2017; 69: 34–40.
 24. Xu ME, Xiao SZ, Sun YH, et al. Effects of astragaloside IV on pathogenesis of metabolic syndrome in vitro. *Acta Pharmacol Sin* 2006; 27: 229–236.
 25. Zhao Z, Wang W, Wang F, et al. Effects of Astragaloside IV on heart failure in rats. *Chin Med* 2009; 4: 6.
 26. Zhang N, Wang XH, Mao SL, et al. Astragaloside IV improves metabolic syndrome and endothelium dysfunction in fructose-fed rats. *Molecules* 2011; 16: 3896–3907.
 27. He Y, Xi J, Zheng H, et al. Astragaloside IV inhibits oxidative stress-induced mitochondrial permeability transition pore opening by inactivating GSK-3 β via nitric oxide in H9c2 cardiac cells. *Oxid Med Cell Longev* 2012; 2012: 935738.
 28. Fu S, Zhang J, Menniti-Ippolito F, et al. Huangqi injection (a traditional Chinese patent medicine) for chronic heart failure: a systematic review. *PLoS One* 2011; 6: e19604.
 29. Liu TP, Lee CS, Liou SS, et al. Improvement of insulin resistance by *Acanthopanax senticosus* root in fructose-rich chow-fed rats. *Clin Exp Pharmacol Physiol* 2005; 32: 649–654.
 30. Zhao J, Yang P, Li F, et al. Therapeutic effects of astragaloside IV on myocardial injuries: multi-target identification and network analysis. *PLoS One* 2012; 7: e44938.

31. Xu XL, Chen XJ, Ji H, et al. Astragaloside IV improved intracellular calcium handling in hypoxia-reoxygenated cardiomyocytes via the sarcoplasmic reticulum Ca-ATPase. *Pharmacology* 2008; 81: 325–332.
32. Davel AP, Victorio JA, Delbin MA, et al. Enhanced endothelium-dependent relaxation of rat pulmonary artery following β -adrenergic overstimulation: involvement of the NO/cGMP/VASP pathway. *Life Sci* 2015; 125: 49–56.
33. Zhang WD, Zhang C, Wang XH, et al. Astragaloside IV dilates aortic vessels from normal and spontaneously hypertensive rats through endothelium-dependent and endothelium-independent ways. *Planta Med* 2006; 72: 621–626.
34. Zhang C, Wang XH, Zhong MF, et al. Mechanisms underlying vasorelaxant action of astragaloside IV in isolated rat aortic rings. *Clin Exp Pharmacol Physiol* 2007; 34: 387–392.
35. van Heerebeek L, Hamdani N, Falcao-Pires I, et al. Low myocardial protein kinase G activity in heart failure with preserved ejection fraction. *Circulation* 2012; 126: 830–839.
36. Brutsaert DL. Cardiac endothelial-myocardial signaling: its role in cardiac growth, contractile performance, and rhythmicity. *Physiol Rev* 2003; 83: 59–115.
37. Chang JC, Wu MC, Liu IM, et al. Increase of insulin sensitivity by stevioside in fructose-rich chow-fed rats. *Horm Metab Res* 2005; 37: 610–616.
38. Xi L, Qian Z, Xu G, et al. Beneficial impact of crocetin, a carotenoid from saffron, on insulin sensitivity in fructose-fed rats. *J Nutr Biochem* 2007; 18: 64–72.
39. Bostick B, Habibi J, Ma L, et al. Dipeptidyl peptidase inhibition prevents diastolic dysfunction and reduces myocardial fibrosis in a mouse model of Western diet induced obesity. *Metabolism* 2014; 63: 1000–1011.
40. Franssen R, Monajemi H, Stroes ES, et al. Obesity and dyslipidemia. *Med Clin North Am* 2011; 95: 893–902.
41. Kurukulasuriya LR, Stas S, Lastra G, et al. Hypertension in obesity. *Med Clin North Am* 2011; 95: 903–917.
42. Roberts CK, Barnard RJ, Sindhu RK, et al. Oxidative stress and dysregulation of NAD(P)H oxidase and antioxidant enzymes in diet-induced metabolic syndrome. *Metabolism* 2006; 55: 928–934.
43. Bir SC, Pattillo CB, Pardue S, et al. Nitrite anion therapy protects against chronic ischemic tissue injury in db/db diabetic mice in a NO/VEGF-dependent manner. *Diabetes* 2014; 63: 270–281.
44. Jia G and Sowers JR. New thoughts in an old player: role of nitrite in the treatment of ischemic revascularization. *Diabetes* 2014; 63: 39–41.
45. Faria AM, Papadimitriou A, Silva KC, et al. Uncoupling endothelial nitric oxide synthase is ameliorated by green tea in experimental diabetes by re-establishing tetrahydrobiopterin levels. *Diabetes* 2012; 61: 1838–1847.
46. Taverne YJ, de Beer VJ, Hoogteijling BA, et al. Nitroso-redox balance in control of coronary vasomotor tone. *J Appl Physiol (1985)* 2012; 112: 1644–1652.